NASA/TM—2014-218412

Atomic Oxygen Energy in Low Frequency Hyperthermal Plasma Ashers

Bruce A. Banks
Science Application International Corporation, Cleveland, Ohio

Christian A. Kneubel
BAB Technology, LLC, Olmsted Township, Ohio

Sharon K. Miller
Glenn Research Center, Cleveland, Ohio

November 2014

NASA STI Program . . . in Profile

Since its founding, NASA has been dedicated to the advancement of aeronautics and space science. The NASA Scientific and Technical Information (STI) program plays a key part in helping NASA maintain this important role.

The NASA STI Program operates under the auspices of the Agency Chief Information Officer. It collects, organizes, provides for archiving, and disseminates NASA's STI. The NASA STI program provides access to the NASA Aeronautics and Space Database and its public interface, the NASA Technical Reports Server, thus providing one of the largest collections of aeronautical and space science STI in the world. Results are published in both non-NASA channels and by NASA in the NASA STI Report Series, which includes the following report types:

- TECHNICAL PUBLICATION. Reports of completed research or a major significant phase of research that present the results of NASA programs and include extensive data or theoretical analysis. Includes compilations of significant scientific and technical data and information deemed to be of continuing reference value. NASA counterpart of peer-reviewed formal professional papers but has less stringent limitations on manuscript length and extent of graphic presentations.

- TECHNICAL MEMORANDUM. Scientific and technical findings that are preliminary or of specialized interest, e.g., quick release reports, working papers, and bibliographies that contain minimal annotation. Does not contain extensive analysis.

- CONTRACTOR REPORT. Scientific and technical findings by NASA-sponsored contractors and grantees.

- CONFERENCE PUBLICATION. Collected papers from scientific and technical conferences, symposia, seminars, or other meetings sponsored or cosponsored by NASA.

- SPECIAL PUBLICATION. Scientific, technical, or historical information from NASA programs, projects, and missions, often concerned with subjects having substantial public interest.

- TECHNICAL TRANSLATION. English-language translations of foreign scientific and technical material pertinent to NASA's mission.

Specialized services also include creating custom thesauri, building customized databases, organizing and publishing research results.

For more information about the NASA STI program, see the following:

- Access the NASA STI program home page at *http://www.sti.nasa.gov*

- E-mail your question to *help@sti.nasa.gov*

- Fax your question to the NASA STI Information Desk at 443–757–5803

- Phone the NASA STI Information Desk at 443–757–5802

- Write to:
  STI Information Desk
  NASA Center for AeroSpace Information
  7115 Standard Drive
  Hanover, MD 21076–1320

NASA/TM—2014-218412

Atomic Oxygen Energy in Low Frequency Hyperthermal Plasma Ashers

Bruce A. Banks
Science Application International Corporation, Cleveland, Ohio

Christian A. Kneubel
BAB Technology, LLC, Olmsted Township, Ohio

Sharon K. Miller
Glenn Research Center, Cleveland, Ohio

National Aeronautics and
Space Administration

Glenn Research Center
Cleveland, Ohio 44135

November 2014

Level of Review: This material has been technically reviewed by technical management.

Available from

NASA Center for Aerospace Information
7115 Standard Drive
Hanover, MD 21076–1320

National Technical Information Service
5301 Shawnee Road
Alexandria, VA 22312

Available electronically at http://www.sti.nasa.gov

Atomic Oxygen Energy in Low Frequency Hyperthermal Plasma Ashers

Bruce A. Banks
Science Application International Corporation
Cleveland, Ohio 44135

Christian A. Kneubel
BAB Technology, LLC
Olmsted Township, Ohio 44138

Sharon K. Miller
National Aeronautics and Space Administration
Glenn Research Center
Cleveland, Ohio 44135

Abstract

Experimental and analytical analysis of the atomic oxygen erosion of pyrolytic graphite as well as Monte Carlo computational modeling of the erosion of Kapton H (DuPont, Wilmington, DE) polyimide was performed to determine the hyperthermal energy of low frequency (30 to 35 kHz) plasma ashers operating on air. It was concluded that hyperthermal energies in the range of 0.3 to 0.9 eV are produced in the low frequency air plasmas which results in texturing similar to that in low Earth orbit (LEO). Monte Carlo computational modeling also indicated that such low energy directed ions are fully capable of producing the experimentally observed textured surfaces in low frequency plasmas.

Introduction

Radio frequency (RF - 13.56 MHz) plasma ashers have been highly successful in identifying the suitability of atomic oxygen protective coatings for low Earth orbital (LEO) spacecraft materials such as the solar array blankets on the International Space Station (Refs. 1 to 3). However, recent atomic oxygen durability experiments performed in low frequency (LF - 30 to 35 kHz) plasma ashers have shown to be much more accurate predictors of the in-space atomic oxygen erosion yield (volume removed per incident atom) than thermal energy plasma ashers (Refs. 4 to 6). It is thought that the arrival flux is much more directed in LF ashers and at normal incidence as opposed to the RFs plasma ashers which produce a more isotropic arrival flux. Comparing the surface texture of polymers resulting from thermal energy exposure with hyperthermal energy, there is a visible increase in height-to-width aspect ratio of the surface features. This is also thought to give rise to large differences in atomic oxygen erosion yield for polymers with significant amounts of inorganic fill such as ash or pigment particles (Ref. 4). Figure 1 compares the surface texture of chlorotrifluoroethylene exposed to thermal energy atomic oxygen (~0.04 eV) in a RF air plasma with hyperthermal (~4.5 eV) atomic oxygen in LEO.

The LF plasma ashers have consistently shown the development of higher aspect ratio textures on polymers than the RF plasma ashers indicating that the arriving atomic oxygen may be more directed and potentially at higher energies. This paper reports the results of tests conducted to confirm the directionality and measure the approximate energy of arriving atomic oxygen in LF plasmas.

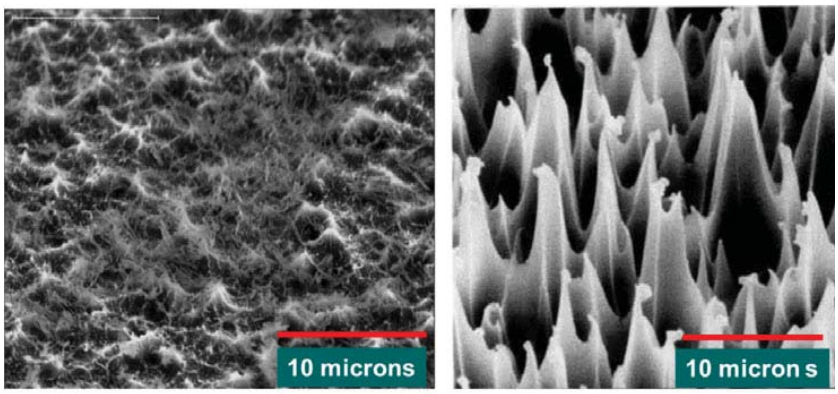

(a) (b)

Figure 1.—Scanning electron microscope images of atomic oxygen textured chlorotrifluoroethylene exposed to a fluence of: (a) 1.25×10^{21}atoms/cm^2 in a thermal energy plasma and (b) 8.99×10^{21} atoms/cm^2 at ~4.5 eV in LEO on the Long Duration Exposure Facility.

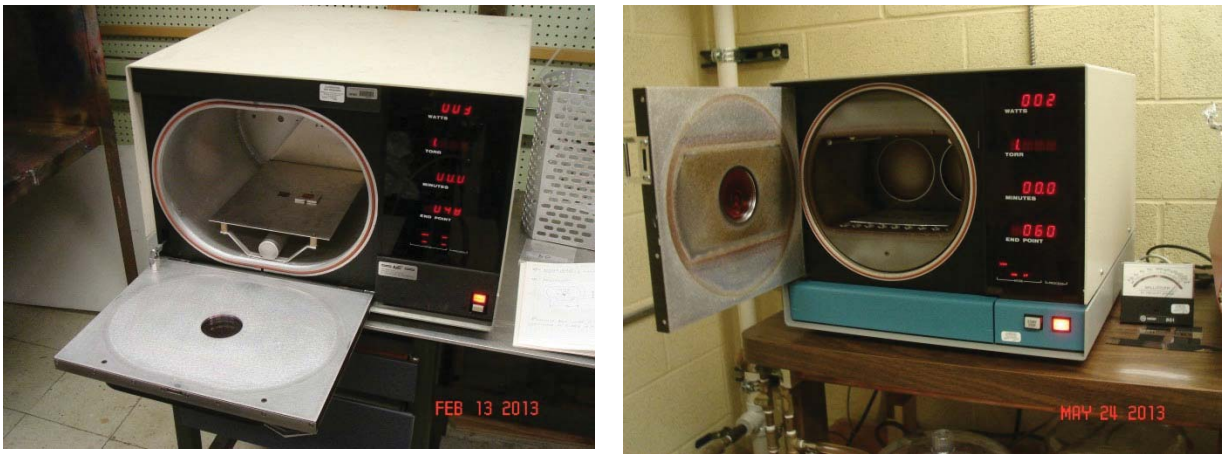

(a) (b)

Figure 2.—LF plasma ashers: (a) LF-6, 30 kHz and (b) LF-5, 35 kHz.

Apparatus and Procedure

Apparatus

Experiments were conducted in two different LF plasma ashers operated on air at a pressure of ~150 millitorr and a power of 35 W are shown in Figure 2.

Preliminary tests of pyrolytic graphite placed in an aluminum box with a slit opening in the top produced a clear band of atomic oxygen textured graphite below the slit. This was clear indication that the preponderance of the atomic oxygen arrival was highly directed. In a thermal energy asher there would simply be a very distributed indication of arrival. Figure 3 shows the geometry and resulting textured pattern in the pyrolytic graphite target.

As a result of the rather clear definition but narrow textured band, an experiment was constructed to produce a wider and more measurable width textured pyrolytic graphite band by using a greater separation between the slit opening and the pyrolytic graphite below. Figure 4 shows the geometry and resulting texture pattern.

Although the texture is not as contrasting as with the close gap of Figure 3, its width is still reasonably measurable and was used to calculate an approximate range of hyperthermal energies based on various plasma temperature assumptions.

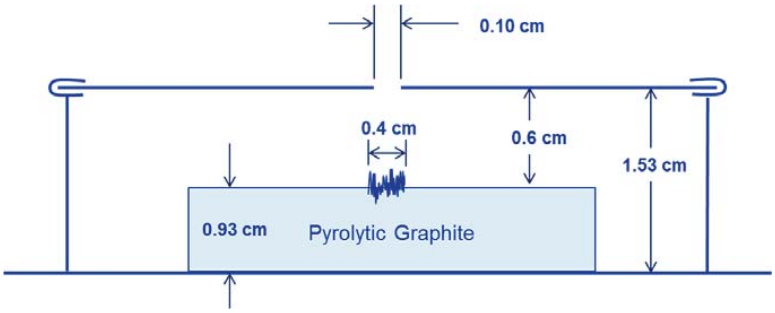

(a)

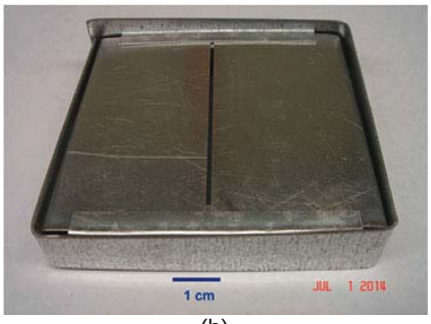

(b)

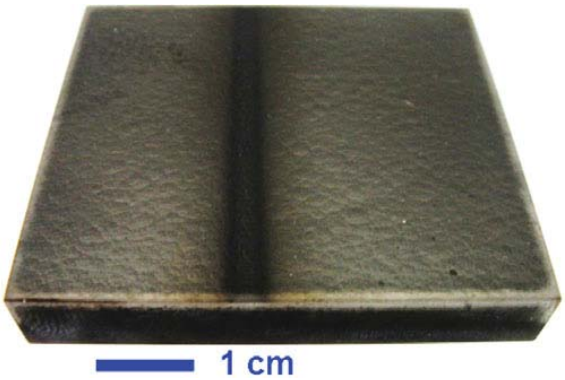

(c)

Figure 3.—Test of pyrolytic graphite in an aluminum box with a slit lid close to the graphite: (a) Exposure geometry, (b) Photograph of test, (c) Resulting texture pattern after exposure in a hyperthermal energy asher.

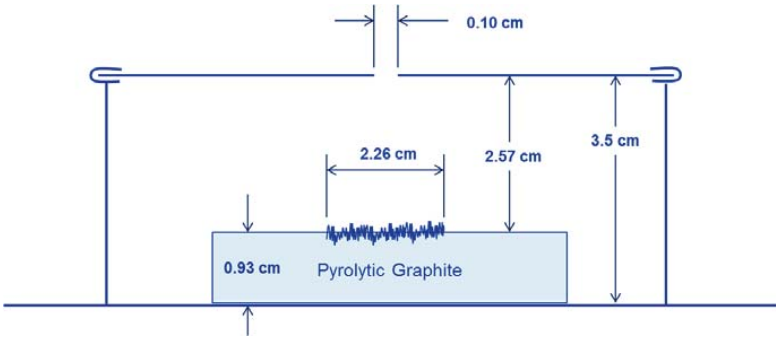

(a)

(b)

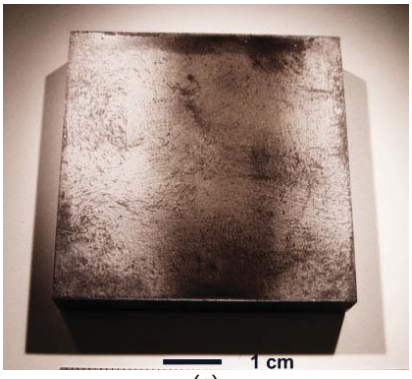

(c)

Figure 4.—Test of pyrolytic graphite in an aluminum box with a slit lid with a greater separation to the graphite: (a) Exposure geometry, (b) Photograph of test, (c) Resulting texture pattern after exposure in a hyperthermal energy asher.

Procedure

The measurement of the hyperthermal ion energy involves estimation of the angular distribution of ions arriving through the slit where the velocity and energy of ions are due to both thermal energy and hyperthermal contributions. As a result of the LF plasma dissociation of the diatomic oxygen molecules, either single oxygen atoms are produced or O_2^+ diatomic oxygen molecules are produced. Measurements of the oxygen O^+ and O_2^+ populations from similar low pressure end Hall oxygen plasmas using E x B probes indicate a neglibile O^+ content and that almost all of the ions are O_2^+ (Ref. 7). If one assumes that the LF plasma creates an O_2^+ ion temperature of T °K then from the equipartition of energy theorem, there is ½ kT of energy for each of three degrees of translational freedom, ½ kT for each of two rotational axes of the diatomic molecule and two vibrational degrees of freedom of the O-O bond, totaling to $\frac{7}{2}kT$ per O_2^+ ion. One can question as to whether the translational, rotational, and vibrational energy have the same consequences of contributing to oxidative erosion as would a monotonic O^+ ion of the same total energy, however it is probable that energy (whether kinetic, rotational, or vibrational) is all deposited upon impact and that all contribute similarly to the erosion process. This would be true whether or not there is impact dissociation of the O_2^+ ion. Thus the total thermal energy of the atomic oxygen ions (and neutrals) is given by E_T where

$$E_T = \frac{7}{2}\,kT = \frac{1}{2}\,M{v_T}^2 + 2\,kT \tag{1}$$

and

$$\frac{1}{2}\,M{v_T}^2 = \frac{3}{2}\,kT \tag{2}$$

Where M = mass of the O_2^+ ions = 5.32×10^{-26} kg
v_T = Root-mean-squared (rms) thermal velocity of the O_2^+ ions
k = Boltzmann's constant = 1.38×10^{-23} joules/°K

Thus

$$v_T = \sqrt{\frac{3\,k\,T}{M}} \tag{3}$$

The ions formed are accelerated by the low frequency electric field which is only in the up and down direction whereas the thermal velocity vector adds to the hyperthermal electric field in an isotropic manner. Figure 5 shows a schematic of the slit, graphite target, and velocity vector geometries. The rms velocity, v_T, of the thermal velocity vector, V_T, is given by $v_T = |V_T|$ where

$$V_T = v_T\,[(\sin\theta)\hat{\imath} + (\cos\theta)\,\hat{\jmath}] \tag{4}$$

Where $\hat{\imath}$ and $\hat{\jmath}$ are unit vectors in the x and -y directions and θ is the angle of an O_2^+ ion relative to straight downward. The maximum hyperthermal velocity, v_H , is given by $v_H = |V_H|$ where

$$V_H = v_H\,\hat{\jmath} \tag{5}$$

and

$$\frac{1}{2}M\,v_H^2 = eE_H \tag{6}$$

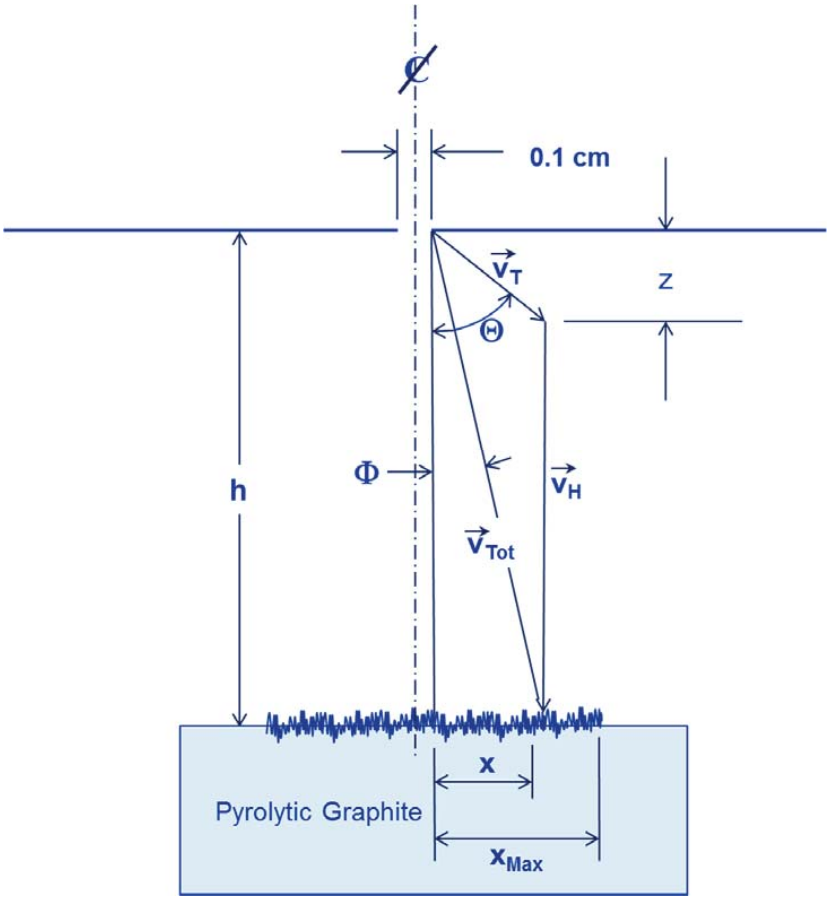

Figure 5.—Schematic of the geometries in the LF plasma asher, where V_T = the thermal velocity vector, V_H = the electric field vector, and V_{Tot} is the total velocity vector.

Thus

$$v_H = \sqrt{\frac{2eE_H}{M}} \tag{7}$$

where

e = electron charge = 1.6×10^{-19} coulombs

E_H = hyperthermal energy due to the acceleration of the O_2^+ ions into the slit opening.

Thus the total velocity vector sum is

$$V_{Tot} = V_T + V_H \tag{8}$$

whose magnitude can be found from Equations (3) to (7).

$$v_{Tot} = \left(\frac{3kT}{M} + \frac{2}{M}\sqrt{6kTeE_H}\,cos\theta + \frac{2eE_H}{M}\right)^{1/2} \tag{9}$$

The total energy, E_{Tot}, of the O_2^+ ions, from Equations (1) and (9) is thus given by

$$E_{Tot} = \frac{7kT}{2} + \sqrt{6kTeE_H}\,cos\theta + eE_H \tag{10}$$

Based on the activation energy (Ref. 8) for an oxygen plasma erosion of carbon, the cosine dependence of atomic oxygen flux through the slit, the arrival of the atomic oxygen at an angle, Φ, with respect to the surface normal, and the loss of flux due to the distance from the slit, the erosion depth, *y*, is given by

$$y \propto e^{-E_0/E_{Tot}} \cos^2 \emptyset \,/\sqrt{h^2 + x^2} \tag{11}$$

where

$E_0 =$ activation energy 0.27 eV = 4.33×10^{-21} joules
$h =$ vertical distance from slit to the top surface of the pyrolytic graphite (see Fig. 5)
$x =$ horizontal distance from the edge of the slit (see Fig. 5)

Based on the velocity vectors orientation and magnitude as well as the geometry shown in Figure 5

$$\cos \emptyset = \frac{h}{\sqrt{x^2 + h^2}} \tag{12}$$

$$\frac{z}{h} = \frac{v_T \cos\theta}{v_T \cos\theta + v_H} \tag{13}$$

and

$$\tan\theta = \frac{x}{z} = \frac{x\,(v_T \cos\theta + v_H)}{h v_T \cos\theta} \tag{14}$$

Solving for θ involves a quadratic equation which results in

$$\sin\theta = \frac{h v_H x \pm x\sqrt{h^2 v_H^2 - (h^2 + x^2)(v_H^2 - v_T^2)}}{v_T(h^2 + x^2)} \tag{15}$$

By using Equation (11) and the related Equations (7), (8), (9), (10), (12), (14), and (15) to plot y versus x one can find a reasonable match between the observed x_{Max} for the specific *h* shown in Figure 5. The choice of the ± in the quadratic equation for sin θ turns out to be not important because it makes only a fraction of 1 percent difference in the resulting erosion.

Results and Discussion

Based on measurements shown in Figure 3, $x_{Max} = 1.08\ cm$ and $h = 2.57\ cm$, and using Equations (11) and its related equations, trials of hyperthermal energies and thermal energy temperatures were assumed which resulted in the plots of erosion depth shown in Figure 6.

The abrupt theoretical discontinuity of the erosion depth near $x_{Max} = 1.08$ cm would not be expected to occur experimentally because we have assumed a single value (the root mean squared value) for the thermal velocity of atoms and ions where in reality there is a Maxwell Boltzmann distribution which would tend to make a smoother transition. The hyperthermal energy shown in Figure 6, of 0.26 eV, is consistent with the observed results shown in Figure 4(b) provided the assumed thermal plasma temperature is 300 °K. If one assumes a different plasma temperature then somewhat different hyperthermal energies result. Because there are two unknowns: hyperthermal energy and temperature of the thermal plasma a plot of hyperthermal energy versus plasma temperature can be made where the erosion stops at $x_{Max} = 1.08$ cm which matches the experimental data. The result is shown in Figure 7. Thus assuming a thermal plasma temperature between 300 and 1000 °K, the hyperthermal energy is between 0.3 and 0.9 eV. This is a factor of ~6.5 higher than for a thermal energy plasma of any temperature but the arrival is from a uniaxial direction which results in a textured surface morphology similar to LEO.

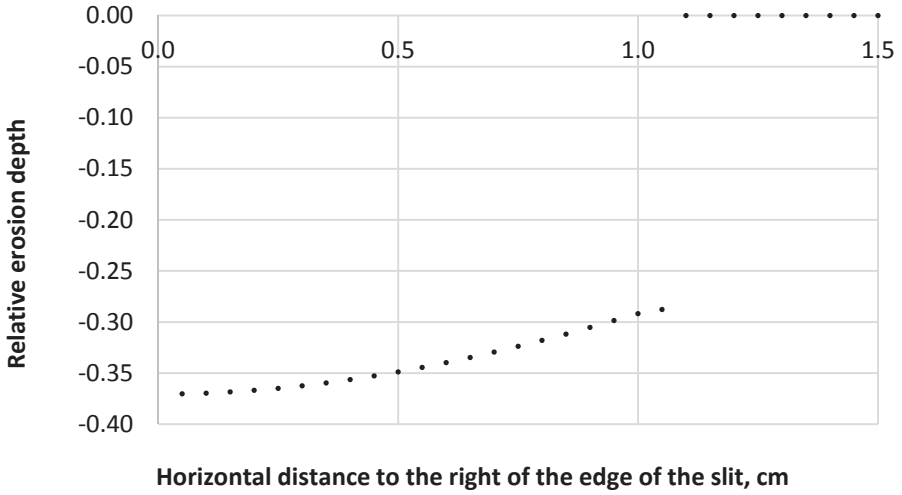

Figure 6.—Predicted erosion depth, y, versus horizontal distance, x for a 300 °K plasma and a hyperthermal energy of 0.26 eV.

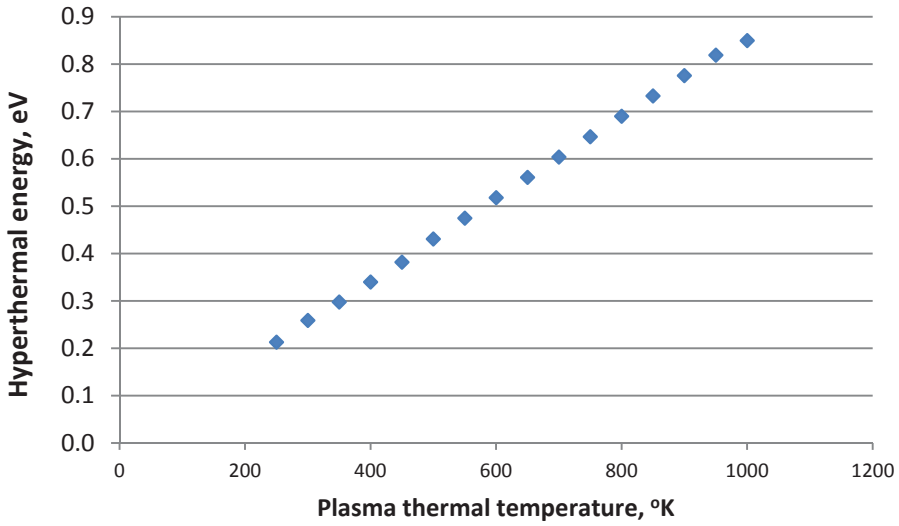

Figure 7.—Predicted hyperthermal energy versus thermal energy plasma temperature.

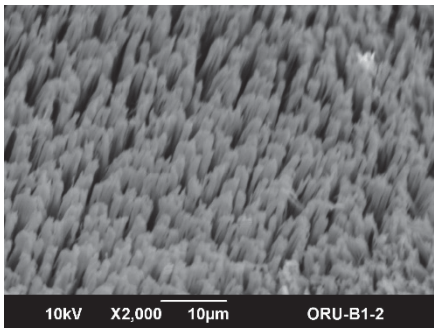

Figure 8.—Scanning electron microscope image of the surface of pyrolytic graphite exposed to atomic oxygen an LF hyperthermal plasma.

Figure 8 contains a scanning electron microscope image of the surface of pyrolytic graphite exposed to the LF hyperthermal plasma. The texture is indicative of the very directed atomic oxygen flux and is much closer to the hyperthermal texture developed in LEO as shown in Figure 1(b) than the cratered surface from thermal energy asher exposure of CTFE in Figure 1(a).

It has been debated whether directed sub-1 eV ions are capable of producing the texture shown in Figure 8 when the thermal energy (0.04 to 0.13 eV) is so close to the hyperthermal energy. Monte Carlo computational model predictions of the eroded surface profile were made using a model that has been developed to mathematically simulate the erosion of polymers by atomic oxygen on Kapton H polyimide (Refs. 9 to 11). The model is a two dimensional array of simulated polymer square cells (1000×1000 cells) that are removed when atomic oxygen oxidizes them. The model allows great flexibility in assumptions so that the interaction parameters can be tuned to replicate observed erosion in a variety of atomic oxygen environments including ram or sweeping hyperthermal low Earth orbital atomic oxygen, or isotropic thermal energy oxygen representative of radio frequency plasma ashers.

In the model, atoms are mathematically impinged upon a test surface in random locations upon a polymer surface or a surface that adjoins a polymer. Upon impact with a non-reactive surface such as aluminum or silicon dioxide, the atomic oxygen can recombine to become chemically inactive or remain atomic and scatter with reduced energy in either a specular, random cosine (Lambertian) direction, or a prescribed direction relative to the local surface normal. If the atoms are scattered, then they have another chance of reacting, recombining, or scattering.

If the atomic oxygen impacts a polymer it can react producing volatile oxides thus causing the removal of a computational cell or it can be ejected without reaction in a similar manner as atoms scattering off of nonreactive materials. An energy dependent reaction probability, P_E, for surfaces with volatile oxides is given by

$$P_E = ce^{-E_A/E} \tag{16}$$

Where c = a proportionality constant depending upon the polymer
E_A = activation energy, eV
E = atomic oxygen impact energy, eV

In addition to energy dependence of reaction there appears to be a reaction probability dependence on the arriving direction relative to the local surface normal direction. This reaction probability dependence, P_C is given by

$$P_C = (\cos\ \beta)^n \tag{17}$$

where β = the angle between the arriving atomic oxygen direction and the local surface normal
n = cosine exponent = 0.5 based on optimization (Ref. 12)

TABLE 1.—MONTE CARLO INTERACTION PARAMETERS (REF. 10)

Interaction parameter	Value
Atomic oxygen initial impact reaction probability	0.09
Activation energy, E_A, in eV for energy dependent reaction probability	0.26
Atomic oxygen reaction probability dependence exponent upon angle of impact, *n*, where the reaction probability = $P_E \bullet (\cos \beta)^n$ where β is the angle between the arrival direction and the local surface normal and P_E is the energy dependent reaction probability at normal incidence	0.5
Probability of atomic oxygen recombination upon impact with protective coating	0.25
Probability of atomic oxygen recombination upon impact with polymer	0.35
Fractional energy loss, *f,* upon impact with polymer	0.45
Fractional energy loss upon impact with protective coating	0.28
Degree of specularity as opposed to diffuse scattering of atomic oxygen upon non-reactive impact with protective coating where 1 = fully specular and 0 = fully diffuse scattering	0.045
Degree of specularity as opposed to diffuse scattering of atomic oxygen upon non-reactive impact with polymer where 1 = fully specular and 0 = fully diffuse scattering	0.5
Temperature for thermally accommodated atomic oxygen atoms, °K	300
Limit of how many bounces the atomic oxygen atoms are allowed to make before an estimate of the probability of reaction is assigned	25
Thermally accommodated energy/actual atom energy for atoms assumed to be thermally accommodated	0.9
Initial atomic oxygen energy, eV	4.5
Thermospheric atomic oxygen temperature, °K	1000
Atomic oxygen arrival plane relative to Earth for a Maxwell-Boltzmann atomic oxygen temperature distribution and an orbital inclination of 28.5°	Horizontal

(a) (b)

Figure 9.—Monte Carlo predicted Kapton H erosion profiles for a: (a) 300 °K thermal energy plasma and (b) 0.26 eV hyperthermal plasma.

An analysis of the results of low Earth orbital (LEO) reaction of atomic oxygen interacting with protected Kapton H at coating defect sites, allowed the Monte Carlo interaction parameters to be optimized to produce erosion prediction results that replicated LEO results (Ref. 10). These interaction parameters were used for simulation of atomic oxygen erosion of Kapton H polyimide and are listed in Table 1.

Figure 9 compares the Monte Carlo predicted Kapton H erosion profiles for a 300 °K thermal energy plasma and a 0.26 eV hyperthermal plasma for the same number of atoms submitted.

This indicates that texturing can be achieved with oxygen atoms arriving at far less than the hyperthermal energy of LEO (~4.5 eV). The directed nature of the atomic oxygen arrival flux is probably a significant cause for the closer simulation of the erosion yield of pigmented polymers such as white Tedlar.

Summary

The atomic oxygen texturing of graphite was experimentally and analytically examined in an effort to quantify the magnitude of hyperthermal energy in low frequency (30 to 35 kHz) plasma ashers. The results indicate hyperthermal energies in the range of 0.3 to 0.9 eV are produced in the low frequency air plasmas unlike high frequency (13.56 MHz) air plasmas in which the energy is more in the thermal range. The hyperthermal energy in the low frequency ashers is a factor of ~6.5 higher energy than for a thermal energy plasma of any temperature, and the arrival is from a uniaxial direction which results in a textured surface morphology similar to LEO. Monte Carlo modeling also indicates that such low energy directed atoms and ions are fully capable of producing the experimentally observed textured surfaces.

References

1. Banks, B.A., Mirtich, M.J., Rutledge, S.K., and Swec, D.M., "Sputtered Coatings for Protection of Spacecraft Polymers," presented at the 11th ICMC Conference, San Diego, California, April 9-13, 1984; published in Thin Solid Films, 127, 1985.
2. Rutledge, S.K., Banks, B.A., DiFilippo, F., Brady, J.A., Dever, T.M., and Hotes, D., "An Evaluation of Candidate Oxidation Resistant Materials for Space Applications in LEO," NASA-TM-100122, presented at the Workshop on Atomic Oxygen Effects sponsored by NASA JPL, Pasadena, California, November 10-11, 1986.
3. Banks, B.A., Miller, S.K., and de Groh, K., "Low Earth Orbital Atomic Oxygen Interactions with Materials," paper presented at the Second International Energy Conversion Engineering Conference sponsored by the American Institute of Aeronautics and Astronautics, AIAA-2004-5638, NASA TM -2004-213223, Providence, Rhode Island, August 16-19, 2004.
4. Banks, B.A., Simmons, J.C., de Groh, K.K., Miller, S.K., "The Effect of Ash and Inorganic Pigment Fill on the Atomic Oxygen Erosion of Polymers and Paints," Proceedings of the "12th International Symposium on Materials in the Space Environment (ISMSE 12)," Noordwijk, The Netherlands (ESA SP-705, February 2013).
5. Stambler, A. Inoshita, K., Roberts, L., Barbagallo, C., de Groh, K., and Banks, B., "Ground-Laboratory to In-Space Atomic Oxygen Correlation for the Polymer Erosion and Contamination Experiment (PEACE) Polymers," NASA/TM—2011-216904, Jan. 2011.
6. Banks, B.A., Dill, G.C., Loftus, R.J., deGroh, K.K., and Miller, S.K., "Comparison of Hyperthermal Ground Laboratory Atomic Oxygen Erosion Yields With Those in Low Earth Orbit," NASA/TM—2013-216613, December 2013.
7. Rutledge, S.K., Dever, J.A., Banks, B.A., and Olle, R.M., "The Impact of Negative Grounding of Solar Arrays on the Sputtering of Array Surfaces in LEO," presented at the ASME International Solar Energy Conference on Space Solar Power for Orbital and Lunar Applications, Lahaina, Maui, Hawaii, April 4-8, 1992.
8. Banks, B., Miller, S., de Groh, K., and Demko, R., "Atomic Oxygen Effects on Spacecraft Materials," NASA/TM—2003-212484, June 2003 and Proceedings of the 9th International Symposium on Materials in a Space Environment, Noordwijk, The Netherlands, June 16-20, 2003, ESA SP-540, September 2003.
9. Banks, B.A., Auer, B.M., Rutledge, S.K., Gebauer, L., and Sechkar, E.A., "Monte Carlo Modeling of Atomic Oxygen Interaction with Protected Polymers for Projection of Materials Durability in Low Earth Orbit," Proceedings of the MRS 1992 Spring Meeting, San Francisco, California, April 27-May 1, 1992.
10. Banks, B.A. and Stueber, T.J., "Monte Carlo Computational Techniques for Prediction of Atomic Oxygen Erosion of Materials," presented at the NATO Advanced Research Workshop on Computer Modeling of Electronic and Atomic Processes in Solids, Wroclaw, Poland, May 20-23, 1996, published in Computer Modeling of Electronic and Atomic Processes in Solids, Proceedings of the NATO Workshop, edited by R.C. Tennyson & A.E. Kiv, Kluwer Academic Publishing, 1997.
11. B. Banks, T. Stueber, and M. Norris, "Monte Carlo Computational Modeling of the Energy Dependence of Atomic Oxygen Undercutting of Protected Polymers," NASA TM 1998-207423, Fourth International Space Conference, ICPMSE-4, Toronto, Canada, April 23-24, 1998.
12. Banks, B., Miller, S., de Groh, K., and Demko, R., "Atomic Oxygen Effects on Spacecraft Materials," NASA/TM—2003-212484, June 2003 and Proceedings of the 9th International Symposium on Materials in a Space Environment, Noordwijk, The Netherlands, June 16-20, 2003, ESA SP-540, September 2003.